

Durian Shell-Mediated Simple Green Synthesis of Nanocopper against Plant Pathogenic Fungi

Nhat Linh Duong, Van Minh Nguyen, Thi A Ni Tran, Thi Diem Trinh Phan, Thi Bao Yen Tran, Ba Long Do, Nguyen Phung Anh, Thi Anh Thu Nguyen, Thanh Gia-Thien Ho,* and Tri Nguyen*



Cite This: *ACS Omega* 2023, 8, 10968–10979



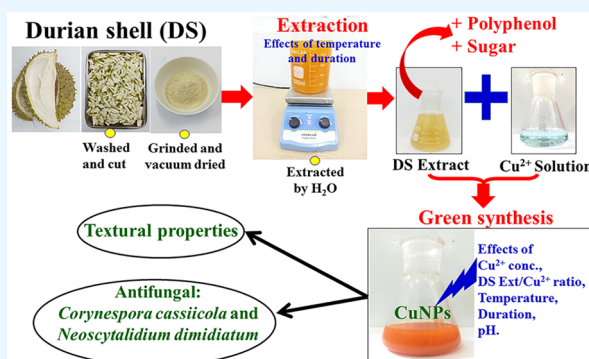
Read Online

ACCESS |

Metrics & More

Article Recommendations

ABSTRACT: The synthesis of fungicides in eco-friendly and cost-effective ways is significantly essential for agriculture. Plant pathogenic fungi cause many ecological and economic issues worldwide, which must be treated with effective fungicides. Here, this study proposes the biosynthesis of fungicides, which combines copper and Cu₂O nanoparticles (Cu/Cu₂O) synthesized using durian shell (DS) extract as a reducing agent in aqueous media. Sugar and polyphenol compounds contained in DS, as the main phytochemicals acting in the reduction procedure, were extracted under different temperatures and duration conditions to obtain the highest yields. We confirmed the extraction process performed at 70 °C for 60 min to be the most effective in extracting sugar (6.1 g/L) and polyphenols (22.7 mg/L). We determined the suitable conditions for Cu/Cu₂O synthesis using a DS extract as a reducing agent for a synthesis time of 90 min, a volume ratio of DR extract/Cu²⁺ of 15:35, an initial pH solution of 10, a synthesis temperature of 70 °C, and a CuSO₄ concentration of 10 mM. The characterization results of as-prepared Cu/Cu₂O NP showed a highly crystalline structure of Cu₂O and Cu with sizes estimated in the range of 40–25 nm and 25–30 nm, respectively. Through in vitro experiments, the antifungal efficacy of Cu/Cu₂O against *Corynespora cassiicola* and *Neoscytalidium dimidiatum* was investigated by the inhibition zone. The green-synthesized Cu/Cu₂O nanocomposites, which are potential antifungals against plant pathogens, exhibited excellent antifungal efficacy against both *Corynespora cassiicola* (MIC = 0.25 g/L, the diameter of the inhibition zone was 22.00 ± 0.52 mm) and *Neoscytalidium dimidiatum* (MIC = 0.0625 g/L, the diameter of the inhibition zone was 18.00 ± 0.58 mm). Cu/Cu₂O nanocomposites prepared in this study could be a valuable suggestion for the control of plant pathogenic fungi affecting crop species globally.



INTRODUCTION

Diseases on crops in general and diseases caused by fungi, in particular, are one of the causes of severe damage to agricultural production.^{1–3} Fungi exist in soil, postharvest residues, water, and air. Pathogenic fungi can survive for a very long time, even in the absence of host plants. They are preserved by mycelium, sclerotia, post scores, egg spores, and thick-walled spores in the soil and on plant residues.⁴ The fungus enters the plant mainly through open wounds, through the vascular cells of the plant that are no longer able to absorb water and nutrients from the substrate. They are always present in the plant but only appear to cause disease at sufficient density. During outbreaks, they reproduce very quickly, causing serious damage.

Corynespora cassiicola is a fungal phytopathogen that affects over 300 plant species and causes significant economic losses in tropical and subtropical countries.⁵ It is an *Ascomycota* that belongs to the *Dothideomycetes* and forms a different phylogenetic group within the *Pleosporales* with *Corynespora*

smithii.⁶ *Corynespora cassiicola* causes the Corynespora Leaf Fall (CLF) disease in rubber trees, which is one of the most serious cryptogamic diseases in rubber plantations.⁷ It was isolated in 1936 in rubber plantations in Sierra Leone and was later discovered in India and Malaysia in the early 1960s.⁷ Since then, the disease has swiftly expanded over most rubber-producing nations in Asia and Africa, causing severe occasional outbreaks and significant losses in natural rubber output. It is a necrotrophic pathogen that colonizes the rubber tree by secreting phytotoxic compounds.⁸ Rubber tree isolates can infect other plants through a selective host range.⁹

Received: November 25, 2022

Accepted: March 6, 2023

Published: March 13, 2023



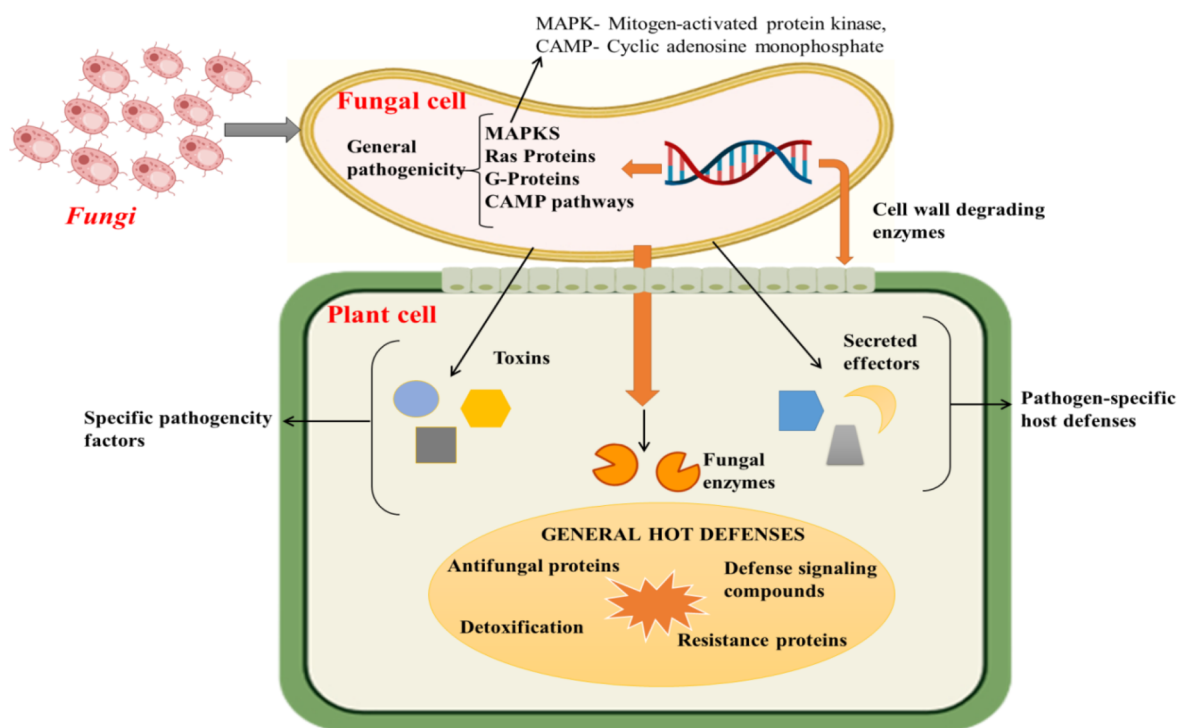


Figure 1. A schematic representation of the fungal pathogenicity effectors, signal transduction pathways activated (MAPK, Mitogen-activated protein kinase; CAMP, cyclic adenosine monophosphate), and host defensive reaction.

Furthermore, the severity of symptoms elicited by a particular isolate varies according to cultivar preferences.¹⁰

In addition, dragon fruit (*Hylocereus undatus*) has a significant export value and is mostly grown in Vietnam. The appearance of brown spot disease caused by *Neoscytalidium dimidiatum* has hampered the production of dragon fruit plants in recent years.¹¹ Until now, appropriate fungicides for managing this disease, which damages the plant cell wall and decreases export economies, have not been discovered. The brown spot disease often emerges during the rainy season, with an infected area of up to 90% and a disease rate of 10–50%.

The mechanism of effectors in plant–fungal interactions is represented in Figure 1. Fungal pathogens attack the hosts using both universal and pathogen-specific pathogenicity mechanisms.¹² Cellular signaling pathway components might be universal pathogenicity factors, which are frequently essential for healthy growth, and fungal enzymes were utilized for plant cell wall disintegration.^{13,14} Plant cell walls are mostly made of cellulose, xylan, and pectin, which act as a natural barrier for plants, preventing disease invasion.¹⁵ Plant pathogens have been shown to produce a series of cell-wall-degrading enzymes (CWDEs) during the mutual recognition process with the host, including cellulase (CL), neutral xylanase (NEX), and polygalacturonase (PG), and these enzymes can degrade plant tissues to provide nutrition for the pathogens and promote their invasion into host tissues.^{16,17} One or a few related fungi species use distinct virulence factors, which may include host-specific poisons and secreted effectors.¹⁸ The host plant's counter-defense mechanisms can be both general (e.g., synthesis of antifungal proteins and activation of defensive signaling pathways) and pathogen-specific (e.g., detoxification of pathogen-specific toxins and specific recognition of pathogen effectors by plant resistance gene products).¹⁹

Therefore, in agricultural production, the treatment of fungal diseases is an urgent requirement. Among the methods of plant-pathogen control, the use of specific topical fungicides is the most common.¹ However, pathogenic fungi can develop different defenses against fungicides. It means that plant pathogenic fungi can adapt to fungicides by mutating, leading to the ineffectiveness of fungicides.²⁰ In addition, the use of toxic fungicide preparations can seriously affect human health and other benign organisms. Therefore, the development of long-term effective, environmentally friendly, and cost-effective fungicides is an important goal for researchers.

In recent years, nanotechnology has proposed various options for treating agricultural problems.^{21,22} It has been reported that nanotechnology can improve crop yields by developing nanofertilizers²³ and nanoparticles to treat plant diseases.^{24,25} Various nanoparticles studied for the treatment of plant diseases have yielded desirable effects, thus being considered a new avenue for developing these applications.^{26–28} Copper-based nanoparticles (Cu-based NPs), including metallic copper nanoparticles (Cu) as well as cuprous oxide nanoparticles (Cu₂O) or nanoparticles cupric oxide nanoparticles (CuO), have attracted attention from diverse disciplines due to the widespread use in electronics, catalysts, sensors, and agricultural and medical applications.²⁹ The antifungal activity of Cu-based nanoparticles has long been recognized. Copper nanoparticles and nanorods have been investigated against *Stachybotrys chartarum* and have recorded low minimum inhibitory concentration (MIC) values.³⁰ Promising antifungal activity of Cu nanoparticles against plant pathogenic fungi such as *Curvularia lunata*, *Phoma*, *Fusarium oxysporum*, and *Alternaria alternata* has also been found.³¹ The antifungal activity of CuO nanoparticles has been studied toward the yeast *Saccharomyces cerevisiae*, resulting in relative performance.³² Meanwhile, Cu₂O nanoparticles proved to be more effective against yeast *Saccha-*

romyces cerevisiae.³³ At the same time, the combination of CuNPs and Cu₂ONPs (Cu/Cu₂O) has also been reported to enhance effectiveness against yeast *Saccharomyces cerevisiae*,³³ *Neoscytalidium dimidiatum*,²⁹ and *Pyricularia oryzae*.³⁴ Hence, the synergistic effect of Cu/Cu₂O nanocomposites has brought interest to scientists in studying their antifungal ability.

There are many methods of synthesizing Cu-based nanoparticles, such as hydrothermal,^{35,36} microwave,^{37,38} electrochemical,³⁹ chemical reduction,⁴⁰ etc. But they have limitations such as the use of hazardous chemicals, high energy costs, and complicated operating equipment. Therefore, a green synthesis method that is simple, environmentally friendly, and cost-effective should be proposed to synthesize stable Cu-based nanoparticles. The development of biosynthesis of Cu-based nanoparticles using plant extracts plays an important role because it completely matches the criteria above.^{28,41} Plants are sources of phytochemical components such as polyphenols, terpenoids, flavonoids, alkaloids, saponins, vitamins, polysaccharides, proteins, etc., which act as reducing and stabilizing agents for NP biosynthesis.⁴²

Durian is widely known in Asia, especially in Southeast Asia. The durian shell (DS) is regarded as a byproduct of durian agriculture. According to studies, the durian shell contains many polysaccharides, which are long chains of carbohydrate molecules consisting mainly of D-galacturonic acid and neutral sugars such as α -D-rhamnose, α -D-arabinose, D-galactose, D-glucose, and D-fructose.⁴³ These compounds are considered a potential source of natural antioxidants, especially polyphenols and flavonoids. These components are appropriate for use as highly efficient reducing and stabilizing agents for Cu-based nanoparticle synthesis.⁴⁴ However, no studies have been reported using the DS extract as a reducing and stabilizing agent for the synthesis of Cu/Cu₂O nanocomposites.

In this study, Cu/Cu₂O nanocomposites were synthesized by the reduction of CuSO₄ solution using DS extract as a reducing agent. The influences of the synthesis duration, the volume ratio of DS extract/CuSO₄, pH solution, reaction temperature, and the CuSO₄ concentration on the Cu/Cu₂O formation were evaluated. The antifungal activity of Cu/Cu₂O nanocomposites synthesized under the best conditions will be assessed against plant pathogenic microorganisms, particularly *Corynespora cassiicola* and *Neoscytalidium dimidiatum*.

EXPERIMENTAL SECTION

Materials. The shells of durian (*Durio Zibethinus*) were collected from supermarkets in Ho Chi Minh City. After collecting and washing, the durian shells were cut into pieces and dried at 60 °C to constant mass. Copper(II) sulfate (Cu(SO₄)₂·5H₂O, > 99.9%) and sodium hydroxide (NaOH, > 99.9%) were purchased from Sigma-Aldrich.

Extraction of Durian Shells and Determinations of Total Glucose and Polyphenols. The dried durian shells (DS) were ground into fine powder. In the next step, 10 g of DS powder were mixed into 500 mL of distilled water and then heated to *T* (°C) for *t* minutes under stirring. The effects of temperature (*T* = 65, 70, 75, and 80 °C) and durations (*t* = 30, 60, 90, and 120 min) of the extraction on the yields of the total sugar and polyphenol content were surveyed. The DS extract was filtered and kept at 4 °C for further experiments. The polyphenol concentration in DS extract was determined by the colorimetric method using the Folin-Ciocalteu reagent with gallic acid selected as the calibration standard.⁴⁵ The presence of polyphenol in the solution was determined using a UV–vis

spectrophotometer (UV–1800, Shimadzu) at a wavelength of 760 nm. The total sugar in the durian shell extract was determined using Bertrand's technique,⁴⁶ which is a commonly used commercial method and is precise, simple to use, and inexpensive. The manganometric method is used to analyze the precipitate of cuprous oxide created by the reduction of the copper-alkaline liquid in the presence of reducing sugars. Bertrand's tables show a clear relationship between the amount of potassium permanganate (0.1 N) applied and the sample's reducing sugar concentration.

Green Synthesis and Characterizations of Copper Nanoparticles. The green synthesis of copper nanoparticles was started by adding DS extract and 0.01 M CuSO₄ solution into a 250 mL flask under stirring of 300 rpm. The mixture's pH was adjusted by using NaOH 1 M solution. The color transformation from pale green into dark green occurred in the aqueous phase. The process is further followed by heating the mixture to the desired temperature. The formation of the copper nanoparticles is confirmed by the color change from green to brown. The collected copper nanoparticles were washed by centrifugation with a rotational speed of 6,000 rpm until reaching their neutral pH and redispersed in 96° ethanol solution. Finally, the CuNPs powder was dried in a pure nitrogen flow at 80 °C to prevent the oxidation of copper. The effects of the parameters, such as synthesis time (30, 60, 90, and 120 min), the ratio of DS extract and CuSO₄ solution (25/25, 20/30, 15/35, and 10/40), pH solution (9, 10, and 11), reaction temperature (60, 70, and 80 °C), and CuSO₄ concentration (5, 10, 15 mM) on CuNPs synthesis were surveyed.

A UV–vis spectrometer (UV-1800, Shimadzu) was used to observe the formation of copper nanoparticles at 200–800 nm. The samples were diluted five times before being analyzed. The crystal structure of CuNP powder was determined by X-ray diffraction (XRD), using a Bruker D2 Phaser powder diffractometer with Cu K α radiation of 1.5406 nm wavelength at 40 kV and 30 mA in the range of two θ angles 10–80° and a step size of 0.02°/s. The features of functional groups in DS extract on the copper nanoparticles were explored by Fourier transform infrared spectroscopy (FTIR) using an active Tensor 27-Bruker spectrometer with scanning angle from 400 to 4000 cm⁻¹. The morphology, particle size, and crystal phases were also estimated by high-resolution transmission electron microscopy (HR-TEM) using the JEOL JEM2100 instrument. The size distributions of nanoparticles were determined by TEM result using ImageJ 4.0 software and the technique of dynamic light scattering (DLS) on a Malvern instrument. The morphology of copper nanoparticles was also characterized by scanning electron microscopy (SEM) and energy-dispersive X-ray spectroscopy (EDS) on a JEOL JST-IT 200 instrument. Electrochemical equilibrium on the surfaces and molecular vibrations were determined through zeta potential spectroscopy using a Specifica Horiba SZ-100 instrument. The element analysis of copper nanoparticles was performed by energy dispersive X-ray (EDX) spectroscopy on a Horiba-7593 instrument.

Evaluation of Antifungal Activity. The antifungal activity of copper nanoparticles was screened by agar diffusion method. The standard fungi strains was grown in potato dextrose agar (PDA) at 37 °C for 3–5 days before each experiment to ensure viability and purity. The spore suspension was adjusted with NaCl 0.85% containing 0.1% Tween 80 (v/v) to a concentration of approximately 10⁶ spores/mL and spread on

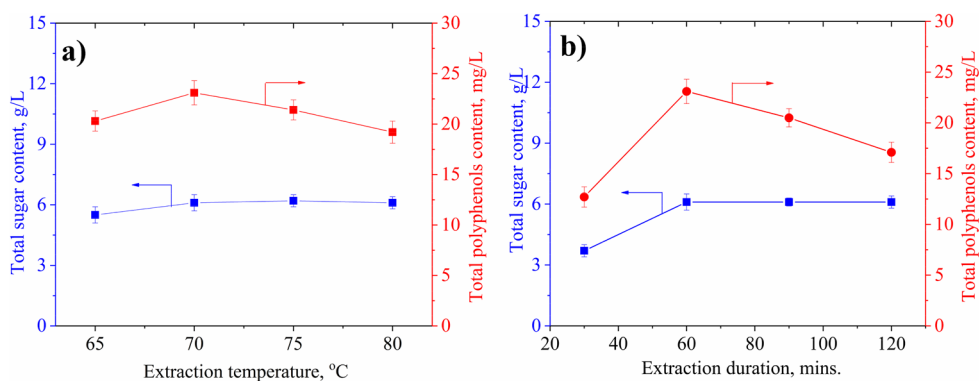


Figure 2. Effects of temperature (a) and duration (b) of durian shell extraction on total sugar and polyphenol content in the extract.

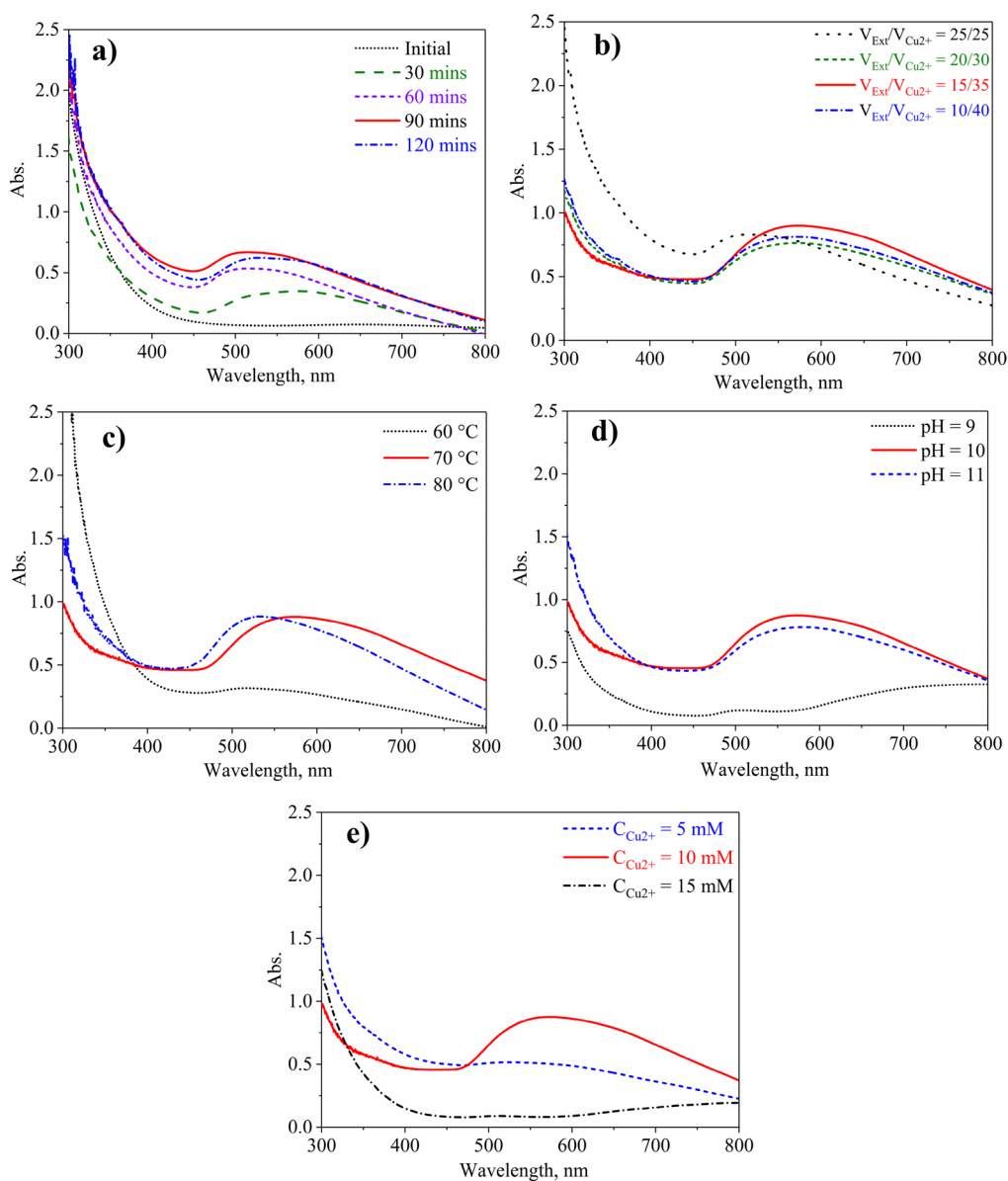


Figure 3. UV-vis spectral analysis of copper nanoparticles under various conditions. (a) Effect of synthesis duration. (b) Effect the volume ratio of DS extract/Cu²⁺. (c) Effect of synthesis temperature. (d) Effect of the initial pH solution. (e) Effect of the CuSO₄ concentration.

PDA plates using sterile cotton swabs, then holes with a diameter of 6 mm were punched on the surface, then 100 μ L of copper nanoparticles were poured into media wells. The

antifungal test plates were incubated at 30 °C for 5 days. After incubation, the diameter of inhibitory zones around each hole was measured. Amphotericin B and sterile potato dextrose

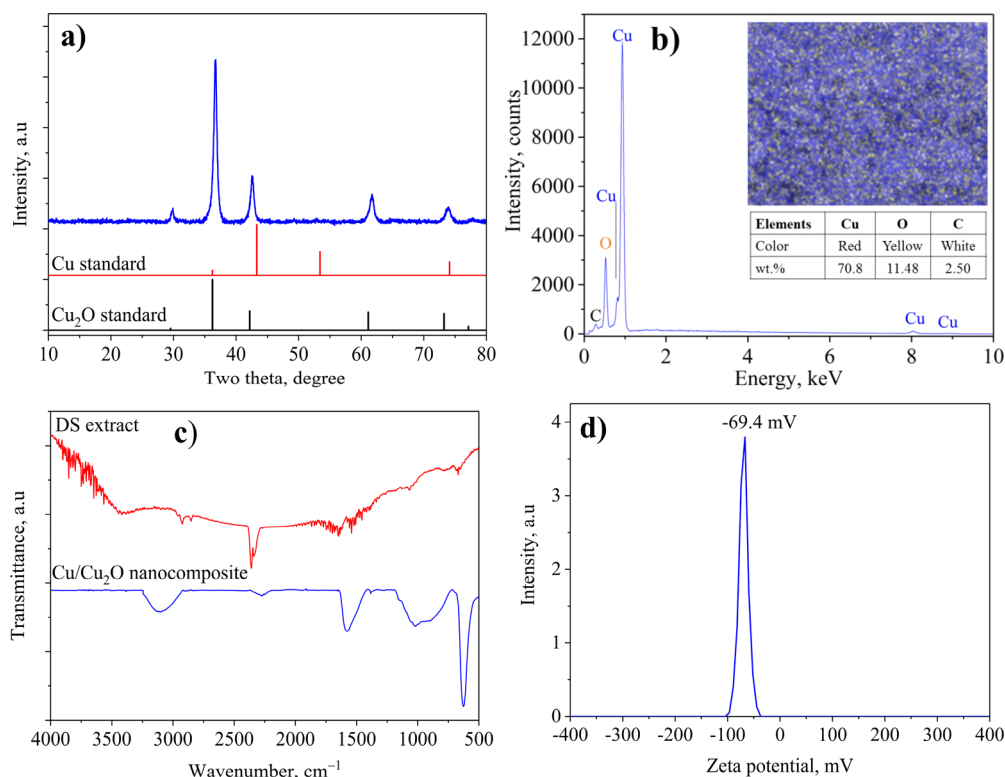


Figure 4. XRD pattern (a), EDS spectrum (b), FT-IR spectra (c), and zeta potential (d) of the sample synthesized under the best conditions.

broth were used as a positive and negative control, respectively. The zone of inhibition was measured (in mm), and three replicates were carried out for the activity of copper nanoparticles against tested fungi.⁴⁷ Additionally, the values of minimum inhibitory concentration (MIC) were determined by the method of dilution in the culture medium.⁴⁸

To ensure accuracy of the results, the tests were undertaken in triplicate. The “mean \pm standard deviation” values were calculated through OriginPro 9.0 software.

RESULTS AND DISCUSSION

The Suitable Extraction of Durian Shell. Experiments were carried out in the range of 65–80 °C at a fixed extraction duration of 60 min to assess the effect of extraction temperature on the generation of total polyphenols and total sugar content from durian shell extract (Figure 2a). At first, the quantity received was marginally tiny. However, increasing the treatment temperature from 65 to 70 °C enhanced the yields, which were highest at 6.1 g/L and 22.7 mg/L, respectively. Furthermore, when the extraction temperatures were raised above 70 °C, there was no substantial rise in phenolic content. The evidence suggests that decomposition of the entire available produced total phenolic compounds from the shell might result in the unchanged yield within this temperature range. These components undergo a chemical transformation when the temperature exceeds the allowable limit and are susceptible to loss through steam entrainment.⁴⁹

The extraction duration of the production of total polyphenols content and total sugar content were also investigated by varying the time from 30–120 min at a fixed reaction temperature of 70 °C. Figure 2b shows the result that the phenolic contents yield increased rapidly to 6.1 g/L and 22.7 mg/L at 60 min, respectively. After this time, production of total polyphenol content almost remained constant, and

total sugar content was decrease significantly. This observation is supported from the previous study.⁵⁰ This might be that the degradation and oxidation of the desired compounds also take place for a prolonged duration, decreasing process efficiency.⁵¹ Hence, the suitable extraction conditions to obtain the highest total sugar and polyphenols content were chosen at 70 °C for 60 min.

Durian Shell-Mediated Green Synthesis of Copper Nanoparticles. The formation of CuNPs was observed by UV–vis spectroscopy, as shown in Figure 3. UV–vis spectra analysis of the synthesized samples showed CuNP formation through the appearance of a peak in the wavelength range of 500–600 nm, discovered after the reaction temperature was kept at 80 °C just after 30 min. When increasing the reaction duration from 30 to 90 min, the CuNP formation increased sharply (Figure 3a). On the other hand, the formation level of CuNPs hardly changed after a reaction time rising up to 120 min; at the same time, the plasmon intensity of the CuNPs synthesized at this time level shifted toward the larger wavelength, indicating that the CuNPs have agglomerated together to form larger-sized particles. Therefore, 90 min is the chosen time to investigate further conditions. With a volume ratio of DS extract/Cu²⁺ of 15:35, the highest performance of CuNPs formation was obtained (Figure 3b). By examining the effect of other parameters, CuNPs were detected with the highest UV–vis absorbance at pH = 10 (see in Figure 3c) and at the temperature of 70 °C (Figure 3d). The effect of CuSO₄ concentration on the CuNPs formation (Figure 3e) showed that the CuNPs concentration grew as the initial Cu²⁺ concentration increased from 5 to 10 mM. The CuNPs formation reduced significantly in the case of continuously rising Cu²⁺ concentration up to 15 mM. The rate of CuNPs formation also increased with increasing Cu²⁺ concentration. However, the newly formed copper nanoparticles can clump

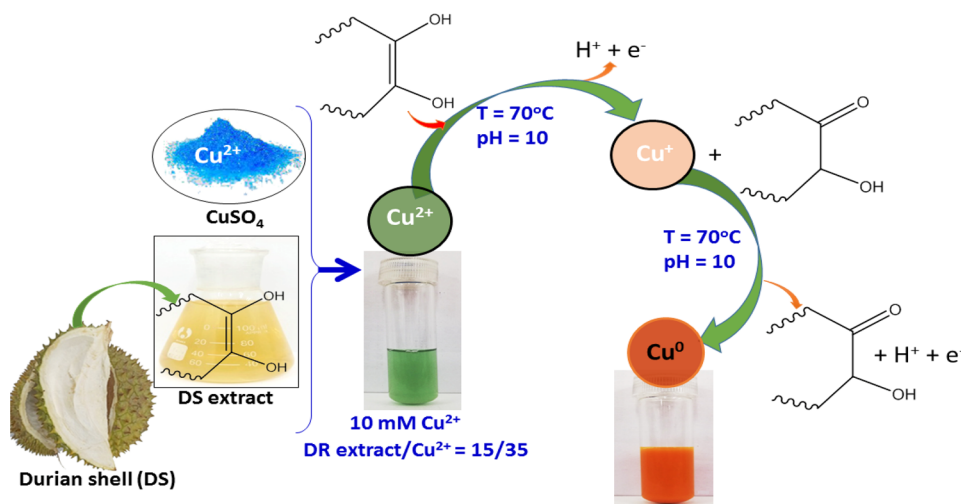


Figure 5. Synthesis mechanism of the CuNP nanocomposite using the DS extract as a reducing agent.

together with too high Cu^{2+} ion concentration, forming larger particles and leading to a decrease in the process's efficiency.

From the results obtained above, the study determined the suitable conditions for CuNPs synthesis using DS extract as a reducing agent in a synthesis time of 90 min, a volume ratio of DS extract/ Cu^{2+} of 15:35, a synthesis temperature of 70 °C, an initial pH solution of 10, and a CuSO_4 concentration of 10 mM.

Characteristics of Copper Nanoparticles. XRD is used to analyze the nature and crystalline phase of Cu/ Cu_2O . The XRD result (Figure 3a) shows diffraction peaks at $2\theta = 29.8, 36.3, 42.2, 61.1, 73.2,$ and 77.1° corresponding to the (110), (111), (200), (220), (311), and (222) planes in the structure of Cu_2O (JCPDS card no. 05-0667). In addition, XRD analysis also showed the presence of Cu at $2\theta = 36.2, 42.6, 50.7,$ and 74.4° , with corresponding lattice planes (111), (111), (200), and (220) of the face-centered cubic structure of zerovalent copper (JCPDS card no. 04-0836). Based on the XRD peaks at 36.3° and 42.6° , the average crystal size of Cu_2O and Cu was calculated based on the Scherrer equation. As a result, the average crystal sizes of Cu_2O and Cu are about 40.5 and 28.3 nm, respectively.

The elemental compositions of the Cu/ Cu_2O nanocomposites were investigated by EDS analysis. The EDS spectrum of the Cu/ Cu_2O sample (Figure 4b) proved the formation of Cu/ Cu_2O nanocomposites with the appearance of Cu and O, and the mass ratio of these elements corresponded to 86.02:11.48. In addition, the peak of C could be related to the presence of phytochemical compounds in the DS extract, as well as the use of carbon tape as a substrate for the preparation of measurement. From XRD and EDS results, we can conclude that Cu/ Cu_2O has been successfully synthesized using DS extract as a reducing agent by the biosynthesis method.

To confirm the creation of Cu/ Cu_2O nanocomposites employing DS extract as a reducing and stabilizing agent, FT-IR analysis was performed. The FT-IR spectrum (Figure 4c) of the DS extract revealed many absorption bands at 3428, 1605, 1442, 1283, 1049, and 671 cm^{-1} corresponding to the functional groups of the plant extract's biomolecules. The broad and strong band at 3428 cm^{-1} is due to polyphenols' hydrogen-bonded OH groups, which are capable of reducing Cu^{2+} ions into CuNPs.^{52,53} The bands at 1605 and 1442 cm^{-1}

are attributable to the C=O stretching of the amide carbonyl and the aromatic amine's C–N stretching vibration.⁵⁴ The C–O–C stretching asymmetric vibration is responsible for a weak band at 1049 cm^{-1} .⁵⁵ In addition, the FT-IR spectroscopy result of the produced Cu/ Cu_2O nanocomposite is presented in Figure 4c. A strong band at 630 cm^{-1} was identified owing to the vibrations of the Cu–O functional group, and a band at 1095 cm^{-1} is linked to the existence of oxygen bonding in copper, confirming the creation of Cu_2O NPs, similar to previous reports.^{56,57} The presence of the carboxylic acid group may be confirmed by the other absorption band at 1200 cm^{-1} .⁵⁸ The C=O stretching of the ketone group was reflected by the peak at 1600 cm^{-1} .⁵⁵ According to FT-IR spectra, the interactions of –OH and C=O groups in the carbohydrates, flavonoids, tannins, and phenolic acids contained in DS may stabilize the produced Cu/ Cu_2O NPs. The mechanism, by which phytochemical compositions performed their function to reduce Cu^{2+} into Cu_2O and Cu phases, is described in Figure 5. The zeta potential in the double electrical layer surrounding CuNPs is -69.4 mV (Figure 4d), confirming their high stability in aqueous solution.

The SEM image established that the CuNP nanocomposite synthesized under suitable conditions was spherical in shape (Figure 6a). It can be observed that the formed Cu_2O particles have a larger size (35–50 nm) than the CuNP particles of smaller size (20–30 nm). The SEAD image shows the appearance of three or four structural planes of Cu_2O next to the smaller CuNPs with two or three planes (Figure 6b). Observing the HRTEM image, it can be seen that the components in the DS extract covered the Cu and Cu_2O particles to prevent their agglomeration. The agglomeration between the spherical particles almost did not occur thanks to the encapsulation of the phytochemical compounds in the DS extract that both act as a reducing agent and prevent their agglomeration after the formation process, thus enhancing the stability of Cu/ Cu_2O nanocomposites. The particle sizes of Cu_2O and Cu have been estimated in the ranges of 40–25 nm and 25–30 nm, respectively (Figure 6c). The *d*-spacings, estimated from SEAD, of 0.25, 0.21, and 0.15 nm (inset Figure 6c) were assigned to (111), (200), and (220) crystal planes of the Cu_2O phase, respectively.⁵⁹ Meanwhile, Cu appears in the (111) and (200) planes with *d*-spacings of 0.21 and 0.18 nm,⁶⁰ and this result also confirmed the formation of Cu^0 , which was

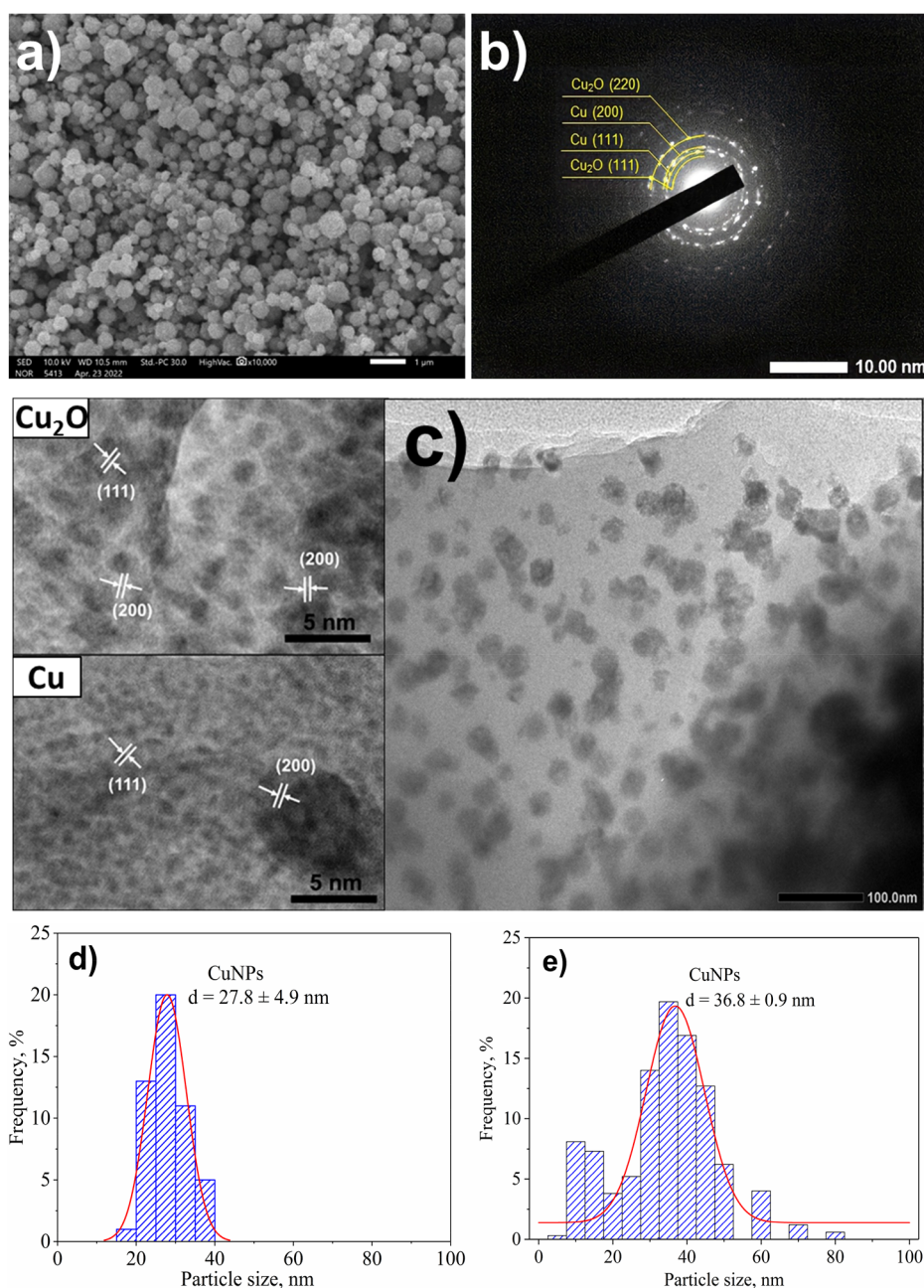


Figure 6. SEM (a), SAED (b), and HRTEM (c) images and the size distributions of nanoparticles using TEM (d) and DLS (e) of the Cu/Cu₂O nanocomposite.

hardly observed in the XRD analysis. From the size distributions of nanoparticles carried out by using TEM images and DLS techniques of the Cu/Cu₂O nanocomposite (Figure 6d,e), the average particle sizes of the sample were demonstrated to be concentrated at 27.8 ± 4.9 nm and 36.8 ± 0.9 nm, respectively. These results are not significantly different, which shows the similarity of two measurements in determining the size of Cu/Cu₂O nanocomposites synthesized green using a DS extract. These results were entirely consistent with the XRD analysis of the sample.

Copper nanoparticles synthesized with different green reducing agents are compared in Table 1. The comparison shows the various size distributions of copper particles affected by the type of reducing and stabilizing agents, parameters of the synthesis process. Though the pH value in synthesizing the

copper nanoparticles by pure (+)-catechin solution was claimed to increase with smaller particle size,⁶¹ some reports show that the suitable pH for the biosynthesis of nanoparticles from a plant extract is in the range of 6–9, while other papers reported the synthesis process in the absence of NaOH or neglecting the pH value in the process (provided information in the Table 1). The varying temperature and interval factor can also be observed in the process of preparing the copper nanoparticles. Some CuNPs were reported to be obtained at room temperature or 1–3 days interval; on the other hand, some were obtained for just 0.25–0.5 h or with the assistance of higher temperature conditions (50–95 °C). The difference in the synthesis procedure may be due to the distinguished content of glucose and polyphenols in each green reducing agent, which is a common feature of green synthesis methods.

Table 1. Comparison of Preparation Conditions and Particle Size of CuNPs Synthesized by Using Various Green Reducing Agents and Copper Precursors

green reducing agents	synthesis conditions	particle size, nm	phase contribution	refs
	CuSO_4			
Durian shell	70 °C, 1.5 h, pH = 10	20–50	Cu/Cu ₂ O	this work
corn starch	50 °C, 3 h	50–100	Cu	63
lemongrass (<i>Cymbopogon citratus</i>)	room temperature, 72 h	2.90 ± 0.64	Cu	64
native cyclodextrins	80 °C, 5 h	2–33	Cu	65
<i>Magnolia kobus</i> leaf	95 °C, 23.3 h	37–110	Cu	66
<i>Bifurcaria bifurcata</i>	100–120 °C, 24 h	5–45	Cu ₂ O/CuO	67
	$\text{Cu}(\text{NO}_3)_2$			
pure (+)-catechin	30 °C, 1 h, pH = 11	3–40	Cu	61
<i>Coffea</i> plant	75 °C for 12 h	262	CuO	68
	CuCl_2			
India neen leaves (<i>Azadirachta indica</i>)	85 °C, 28 h, pH = 6.6	48	Cu	69
<i>Jatropha. curcas</i> leaves	room temperature, 24 h	12 ± 1	Cu	70
<i>Ginkgo biloba</i> Linn leaves	80 °C, 0.5h min, pH = 9	15–20	Cu	71
	$(\text{CH}_3\text{COO})_2\text{Cu}$			
<i>Syzygium aromaticum</i> bud	30 °C, 0.25h	12–15	Cu	72
<i>Eclipta prostrata</i> leaves	50 °C, 0.5 h, pH = 6	28–105	Cu	73

It had been reported that the more phytochemicals that were in the solution to reduce precursor molecules, the faster the rate of nanoparticle formation.⁶² Furthermore, in previous studies, numerous plants with their specific parts were used, resulting in polydisperse CuNPs with vast ranges of variation. When compared to other green reducing agents and precursors, the CuNP sample synthesized from the DS extract and CuSO_4 by the simple technique has a spherical shape, but the synthesis time is greatly reduced, and it has a smaller size and higher uniformity.

Antifungal Activity. The inhibition zones of the synthesized Cu/Cu₂O solution against *Corynespora cassiicola* and *Neoscytalidium dimidiatum* are shown in Figure 7. The results showed that the nanocomposites exhibited good antifungal efficacy against both fungal strains. A wide and relatively heterogeneous inhibition zone was detected, which characterizes the antibacterial ring of fungal strains.^{74–76} The zones of inhibition for *Corynespora cassiicola* and *Neoscytalidium dimidiatum* correspond to 22.00 ± 0.52 mm and 18.00 ± 0.58 mm (Figure 7a,b). And, the extract is not antifungal against both *Corynespora cassiicola* and *Neoscytalidium dimidiatum* (Figure 7c,d). It can be concluded that the biosynthesis of Cu/Cu₂O nanocomposites using durian shell extract as a reducing agent showed high antifungal efficacy against *Corynespora cassiicola* and *Neoscytalidium dimidiatum*. Their excellent antifungal activity can be attributed to the nanoparticle size and the combination of Cu and Cu₂O nanoparticles. For the MIC test (Figure 8), after 5 days of incubation compared with the control, the CuNPs solution could inhibit abilities with *Corynespora cassiicola* and *Neoscytalidium dimidiatum* at the MIC = 0.250 g/L and MIC = 0.0625 g/L, respectively.

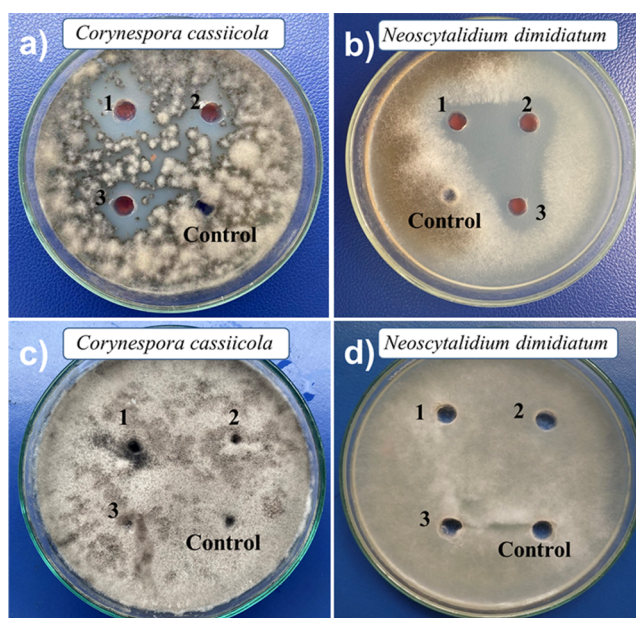


Figure 7. Inhibition zones of synthesized CuNPs solution (a, b) and the DS extract (c, d) against *Corynespora cassiicola* and *Neoscytalidium dimidiatum*.

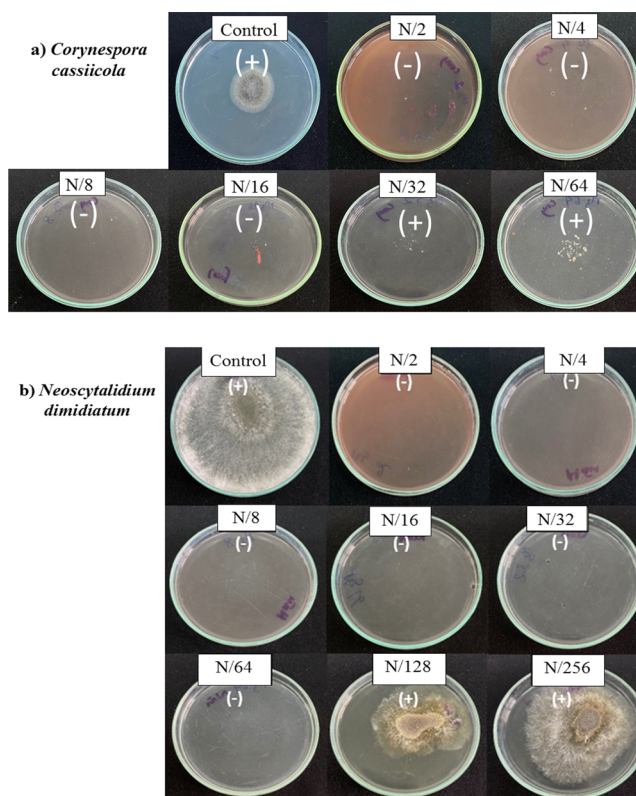


Figure 8. Minimum inhibitory concentration (MIC) of synthesized CuNPs solution against *Corynespora cassiicola* and *Neoscytalidium dimidiatum* ($N = 4.0$ g/L).

Neoscytalidium dimidiatum at the MIC = 0.250 g/L and MIC = 0.0625 g/L, respectively.

The primary goal of Table 2 is to compare the antifungal effects of CuNPs to other nanoparticles against *Neoscytalidium dimidiatum*. It is noticeable that the zone size of the CuNPs sample is larger than that of AgNPs and Ag@CS (as shown in

Table 2. Comparison of Antifungal Activity of the Green Synthesized CuNPs with Other Nanoparticles

samples	IZD, mm	MIC, g/L	refs
CuNPs	22.00 ± 0.52 ^a	0.25 ^a	this work
	18.00 ± 0.58 ^b	0.0625 ^b	
AgNPs	13.33 ± 0.58 ^b	ND	77
Ag@CS	17.42 ± 0.52 ^b	ND	

^a*Corynespora cassiicola*. ^b*Neoscytalidium dimidiatum*. ND, not done.

Table 2); at the same time, this study proposes a simple, economical process for synthesizing copper nanoparticles via green chemistry. Additionally, the inhibition zone diameter of CuNPs against *Corynespora cassiicola* is relatively large. Moreover, to the best of our knowledge, no earlier findings of antifungal activity against *Corynespora cassiicola* employing CuNPs have been published.

In addition, according to Cao et al.,⁷⁸ the synthesized nano copper had strong inhibitory ability against *Corticium salmonicolor*, pathogenic of rubber trees. Pariona et al.²⁸ proposed the green synthesis of fungicides, which consist of copper nanoparticles (CuNPs) prepared in aqueous media; the result proved that the green-synthesized CuNPs are potential fungicides against *F. solani*, *Neofusicoccum* sp., and *F. oxysporum*. Mali et al.²⁰ proposed that the cosynthesized nano sample from *Celastrus paniculatus* was able to inhibit the fungus *Fusarium oxysporum*. Furthermore, the benefits of green synthesis were energy and material savings, as well as environmental friendliness. The technique, in particular, can be carried out at room temperature and advantageously scaled up to mass production at a reasonable cost. On one hand, it aids in the utilization of agricultural waste such as durian shells, while on the other hand, it aids in the development of next generation nanomaterials. As a result, CuNPs appear to be reliable candidates for potentially and effectively suppressing *Corynespora* and *Neoscytalidium dimidiatum*.

Figure 9 depicts the antifungal mechanism of CuNPs against *Corynespora cassiicola* and *Neoscytalidium dimidiatum*, including direct adherence of CuNPs to the fungal surface and the influence on membrane structural integrity.⁷⁹ CuNPs interact with the fungal cell wall due to their affinity for the carboxyl group found on the fungal surface.⁸⁰ The antifungal action of nanoparticles is attributed to the generation of reactive oxygen species (ROS), membrane damage, loss of enzyme activity, protein malfunction, and other factors.⁸⁰ Ashraf et al.

investigated the antifungal behavior of CuNPs.⁸¹ When CuNPs come into contact with a bacterial cell, they release Cu ions, which are absorbed on the cell wall, resulting in the formation of ROS and the loss of membrane integrity.⁸¹ Similarly, CuNPs are also responsible for the disruption of cellular metabolic pathways, the creation of pits in membranes, and the development of oxidative stress, all of which lead to cell death.⁸² The Cu polymer nanocomposite has been presented as an effective antifungal agent. The authors investigated the influence of nanocomposite fungicides on the release of Cu ions and CuNPs.⁸³ When Cu ions engage with the outer fungal membrane, they interact with amines and carboxyl groups in the peptidoglycan layer, as well as sulfhydryl groups, causing protein denaturation.⁸⁴ Cu ions (Cu²⁺) attach to DNA and cross-link nucleic acid strands, resulting in helical structural disorder.⁸⁵ Similarly, the released CuNPs adhere to the cell membrane and enter the fungus via endocytosis.⁸⁶ The sensitivity of microorganisms to the fungicide activity of CuNPs is primarily determined by particle size, electrostatic interaction between microbial cells and nanoparticles, fungal cell wall and membrane composition, and the hydrophobic or hydrophilic character of nanoparticles.⁸⁷

CONCLUSION

Cu/Cu₂O nanocomposites were successfully synthesized by a green method using DS extract as a reducing agent. Sugar and polyphenol compounds contained in DS extract were determined as the main components committing the reduction process. Optimal conditions for extraction, as well as operating parameters for Cu/Cu₂O synthesis, were determined. The Cu/Cu₂O nanocomposites prepared at the optimized conditions were formed as highly crystallized spherical particles and in a size range of 25–40 nm with excellent stability due to the encapsulation of the phytochemical in the DS extract, which prevents the agglomeration of nanoparticles. These green-synthesized Cu/Cu₂O's exhibited excellent antifungal performance against *Corynespora cassiicola* and *Neoscytalidium dimidiatum*. Thus, the nanocomposites prepared in this study could be a valuable suggestion for controlling pathogenic fungi that affect crop species globally.

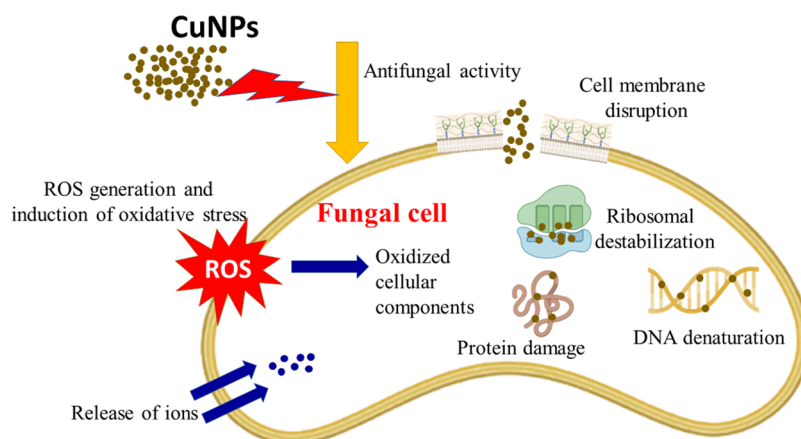


Figure 9. Illustration of antifungal mechanism of CuNPs nanoparticles.

AUTHOR INFORMATION

Corresponding Authors

Thanh Gia-Thien Ho – Institute of Chemical Technology, Vietnam Academy of Science and Technology, Ho Chi Minh City 700000, Vietnam; Email: hogiathienthanh97@gmail.com

Tri Nguyen – Ho Chi Minh City Open University, Ho Chi Minh City 700000, Vietnam; Institute of Chemical Technology, Vietnam Academy of Science and Technology, Ho Chi Minh City 700000, Vietnam; orcid.org/0000-0001-9486-5096; Email: ntri@ict.vast.vn

Authors

Nhat Linh Duong – Ho Chi Minh City Open University, Ho Chi Minh City 700000, Vietnam

Van Minh Nguyen – Ho Chi Minh City Open University, Ho Chi Minh City 700000, Vietnam

Thi A Ni Tran – MIDOLI Company Limited, Ho Chi Minh City 700000, Vietnam

Thi Diem Trinh Phan – Ho Chi Minh City Open University, Ho Chi Minh City 700000, Vietnam

Thi Bao Yen Tran – Ho Chi Minh City Open University, Ho Chi Minh City 700000, Vietnam

Ba Long Do – Institute of Chemical Technology, Vietnam Academy of Science and Technology, Ho Chi Minh City 700000, Vietnam

Nguyen Phung Anh – Institute of Chemical Technology, Vietnam Academy of Science and Technology, Ho Chi Minh City 700000, Vietnam

Thi Anh Thu Nguyen – Tra Vinh University, Tra Vinh City 87000, Vietnam

Complete contact information is available at: <https://pubs.acs.org/10.1021/acsomega.2c07559>

Notes

The authors declare no competing financial interest.

ACKNOWLEDGMENTS

This work was funded by Vingroup Joint Stock Company and supported by Vingroup Innovation Foundation (VINIF) under project code VINIF.2020.NCUD.DA240.

REFERENCES

- (1) Toda, M.; Beer, K. D.; Kuivila, K. M.; Chiller, T. M.; Jackson, B. R. Trends in agricultural triazole fungicide use in the United States, 1992–2016 and possible implications for antifungal-resistant fungi in human disease. *Environ. Health Perspect.* **2021**, *129* (5), 055001.
- (2) Bich, G. A.; Castrillo, M. L.; Kramer, F. L.; Villalba, L. L.; Zapata, P. D. Morphological and molecular identification of entomopathogenic fungi from agricultural and forestry crops. *Floresta Ambient.* **2021**, *28*, e20180086.
- (3) Duarte, P. A.; Menze, L.; Shoute, L.; Zeng, J.; Savchenko, O.; Lyu, J.; Chen, J. Highly efficient capture and quantification of the airborne fungal pathogen *Sclerotinia sclerotiorum* employing a nanoelectrode-activated microwell array. *ACS omega* **2022**, *7* (1), 459–468.
- (4) Campbell, C. K.; Johnson, E. M. *Identification of Pathogenic Fungi*; John Wiley & Sons, 2013.
- (5) Deon, M.; Bourre, Y.; Gimenez, S.; Berger, A.; Bieysse, D.; de Lamotte, F.; Poncet, J.; Roussel, V.; Bonnot, F.; Oliver, G.; Franchel, J.; Seguin, M.; Leroy, T.; Roeckel-Drevet, P.; Pujade-Renaud, V. Characterization of a cassiicolin-encoding gene from *Corynespora cassiicola*, pathogen of rubber tree (*Hevea brasiliensis*). *Plant Science* **2012**, *185*, 227–237.
- (6) Schoch, C.; Crous, P. W.; Groenewald, J. Z.; Boehm, E.; Burgess, T. I.; De Gruyter, J.; De Hoog, G. S.; Dixon, L.; Grube, M.; Gueidan, C.; et al. A class-wide phylogenetic assessment of Dothideomycetes. *Stud. Mycol.* **2009**, *64* (1), 1–15.
- (7) Li, B.; Yang, Y.; Cai, J.; Liu, X.; Shi, T.; Li, C.; Chen, Y.; Xu, P.; Huang, G. Genomic characteristics and comparative genomics analysis of two Chinese *Corynespora cassiicola* strains causing *Corynespora* leaf fall (CLF) disease. *J. Fungi* **2021**, *7* (6), 485.
- (8) Samaco, M. A. *Host-Selective Toxins Produced by Corynespora cassiicola Causing Target Spot Disease in the Southeastern United States*; University of Georgia, 2021.
- (9) Barthe, P.; Pujade-Renaud, V.; Breton, F.; Gargani, D.; Thai, R.; Roumestand, C.; De Lamotte, F. Structural analysis of cassiicolin, a host-selective protein toxin from *Corynespora cassiicola*. *J. Mol. Biol.* **2007**, *367* (1), 89–101.
- (10) Breton, F.; Sanier, C.; D'Auzac, J. Role of cassiicolin, a host-selective toxin, in pathogenicity of *Corynespora cassiicola*, causal agent of a leaf fall disease of Hevea. *J. Rubber Res.* **2000**, *3* (2), 115–128.
- (11) Le Bellec, F.; Vaillant, F.; Imbert, E. Pitahaya (*Hylocereus* spp.): a new fruit crop, a market with a future. *Fruits* **2006**, *61* (4), 237–250.
- (12) Sexton, A. C.; Howlett, B. J. Parallels in fungal pathogenesis on plant and animal hosts. *Eukaryotic Cell* **2006**, *5* (12), 1941–1949.
- (13) Stępień, Ł.; Lalak-Kańczugowska, J. Signaling pathways involved in virulence and stress response of plant-pathogenic Fusarium species. *Fungal Biol. Rev.* **2021**, *35*, 27–39.
- (14) Looi, H. K.; Toh, Y. F.; Yew, S. M.; Na, S. L.; Tan, Y.-C.; Chong, P.-S.; Khoo, J.-S.; Yee, W.-Y.; Ng, K. P.; Kuan, C. S. Genomic insight into pathogenicity of dematiaceous fungus *Corynespora cassiicola*. *PeerJ.* **2017**, *5*, e2841.
- (15) Jia, M.; Liu, X.; Zhao, H.; Ni, Y.; Liu, H.; Tian, B. Cell-wall-degrading enzymes produced by sesame leaf spot pathogen *Corynespora cassiicola*. *J. Phytopathol.* **2021**, *169* (3), 186–192.
- (16) Chen, X.; Lili, L.; Zhang, Y.; Zhang, J.; Ouyang, S.; Zhang, Q.; Tong, Y.; Xu, J.; Zuo, S. Functional analysis of polygalacturonase gene RsPG2 from *Rhizoctonia solani*, the pathogen of rice sheath blight. *Eur. J. Plant Pathol.* **2017**, *149* (2), 491–502.
- (17) Dong, Z.; Wang, Q.; Qin, S.; Wang, Z. Comparison of cell wall degrading enzymes produced by *Fusarium oxysporum* f. sp. cubense race 1 and race 4. *Acta Hydrobiol. Sin.* **2010**, *40* (5), 463–468.
- (18) Doehlemann, G.; Ökmen, B.; Zhu, W.; Sharon, A. Plant pathogenic fungi. *Microbiol. Spectr.* **2017**, *5* (1), 5.1.14.
- (19) Rana, A.; Sahgal, M.; Johri, B. *Fusarium oxysporum*: genomics, diversity and plant–host interaction. In *Developments in Fungal Biology and Applied Mycology*; Springer, 2017; pp 159–199.
- (20) Mali, S. C.; Dhaka, A.; Githala, C. K.; Trivedi, R. Green synthesis of copper nanoparticles using *Celastrus paniculatus* Willd. leaf extract and their photocatalytic and antifungal properties. *Biotechnol. Rep.* **2020**, *27*, e00518.
- (21) Fu, L.; Wang, Z.; Dhankher, O. P.; Xing, B. Nanotechnology as a new sustainable approach for controlling crop diseases and increasing agricultural production. *J. Exp. Bot.* **2020**, *71* (2), 507–519.
- (22) Haris, M.; Hussain, T.; Mohamed, H. I.; Khan, A.; Ansari, M. S.; Tauseef, A.; Khan, A. A.; Akhtar, N. Nanotechnology—A new frontier of nano-farming in agricultural and food production and its development. *Sci. Total Environ.* **2023**, *857*, 159639.
- (23) Preetha, P. S.; Balakrishnan, N. A review of nano fertilizers and their use and functions in soil. *Int. J. Curr. Microbiol. Appl. Sci.* **2017**, *6* (12), 3117–3133.
- (24) Sharon, M.; Choudhary, A. K.; Kumar, R. Nanotechnology in agricultural diseases and food safety. *J. Phytol.* **2010**, *2* (4), 86012960.
- (25) Danish, M.; Altaf, M.; Robab, M. I.; Shahid, M.; Manoharadas, S.; Hussain, S. A.; Shaikh, H. Green synthesized silver nanoparticles mitigate biotic stress induced by *Meloidogyne incognita* in *Trachyspermum ammi* (L.) by improving growth, biochemical, and antioxidant enzyme activities. *ACS Omega* **2021**, *6* (17), 11389–11403.
- (26) Terra, A. L. M.; Kosinski, R. d. C.; Moreira, J. B.; Costa, J. A. V.; Morais, M. G. d. Microalgae biosynthesis of silver nanoparticles for

- application in the control of agricultural pathogens. *J. Environ. Sci. Health - B* **2019**, *54* (8), 709–716.
- (27) Castillo-Henríquez, L.; Alfaro-Aguilar, K.; Ugalde-Álvarez, J.; Vega-Fernández, L.; Montes de Oca-Vásquez, G.; Vega-Baudrit, J. R. Green synthesis of gold and silver nanoparticles from plant extracts and their possible applications as antimicrobial agents in the agricultural area. *Nanomaterials* **2020**, *10* (9), 1763.
- (28) Pariona, N.; Mtz-Enriquez, A. I.; Sánchez-Rangel, D.; Carrión, G.; Paraguay-Delgado, F.; Rosas-Saito, G. Green-synthesized copper nanoparticles as a potential antifungal against plant pathogens. *RSC Adv.* **2019**, *9* (33), 18835–18843.
- (29) Du, B. D.; Ngoc, D. T. B.; Thang, N. D.; Tuan, L. N. A.; Thach, B. D.; Hien, N. Q. Synthesis and in vitro antifungal efficiency of alginate-stabilized Cu₂O-Cu nanoparticles against *Neoscytalidium dimidiatum* causing brown spot disease on dragon fruit plants (*Hylocereus undatus*). *Vietnam J. Chem.* **2019**, *57* (3), 318–323.
- (30) Wei, Y.; Chen, S.; Kowalczyk, B.; Huda, S.; Gray, T. P.; Grzybowski, B. A. Synthesis of stable, low-dispersity copper nanoparticles and nanorods and their antifungal and catalytic properties. *J. Phys. Chem. C* **2010**, *114* (37), 15612–15616.
- (31) Kanhed, P.; Birla, S.; Gaikwad, S.; Gade, A.; Seabra, A. B.; Rubilar, O.; Duran, N.; Rai, M. In vitro antifungal efficacy of copper nanoparticles against selected crop pathogenic fungi. *Mater. Lett.* **2014**, *115*, 13–17.
- (32) Kasemets, K.; Ivask, A.; Dubourguier, H.-C.; Kahru, A. Toxicity of nanoparticles of ZnO, CuO and TiO₂ to yeast *Saccharomyces cerevisiae*. *Toxicol. In Vitro* **2009**, *23* (6), 1116–1122.
- (33) Giannousi, K.; Sarafidis, G.; Mourdikoudis, S.; Pantazaki, A.; Dendrinou-Samara, C. Selective synthesis of Cu₂O and Cu/Cu₂O NPs: antifungal activity to yeast *Saccharomyces cerevisiae* and DNA interaction. *Inorg. Chem.* **2014**, *53* (18), 9657–9666.
- (34) Ngoc, D. T. B.; Du, B. D.; Thach, B. D.; Kien, C. T.; Van Phu, D.; Hien, N. Q. Study on antifungal activity and ability against rice leaf blast disease of nano Cu-Cu₂O/alginate. *Indian J. Agric. Res.* **2020**, *54* (6), 802–806.
- (35) Seku, K.; Reddy Ganapuram, B.; Pejjai, B.; Mangatayaru Kotu, G.; Golla, N. Hydrothermal synthesis of copper nanoparticles, characterization and their biological applications. *Int. J. Nano Dimens.* **2018**, *9* (1), 7–14.
- (36) Zhang, C.; Chen, J.; Chen, W.; Liu, J.; Chen, D. Hydrothermal synthesis of Cu₂O/CuO/hierarchical porous N-doped activated carbon with exceptional electrochemical performance. *J. Energy Storage* **2023**, *60*, 106600.
- (37) El-Berry, M. F.; Sadeek, S. A.; Abdalla, A. M.; Nassar, M. Y. Microwave-assisted fabrication of copper nanoparticles utilizing different counter ions: An efficient photocatalyst for photocatalytic degradation of safranin dye from aqueous media. *Mater. Res. Bull.* **2021**, *133*, 111048.
- (38) Pineda-Castañeda, H. M.; Rivera-Monroy, Z. J.; Maldonado, M. Copper(I)-catalyzed alkyne–azide cycloaddition (CuAAC) “Click” reaction: a powerful tool for functionalizing polyhydroxylated platforms. *ACS Omega* **2023**, *8* (4), 3650–3666.
- (39) Shih, Y.-J.; Wu, Z.-L.; Huang, Y.-H.; Huang, C.-P. Electrochemical nitrate reduction as affected by the crystal morphology and facet of copper nanoparticles supported on nickel foam electrodes (Cu/Ni). *Chem. Eng. J.* **2020**, *383*, 123157.
- (40) Khan, A.; Rashid, A.; Younas, R.; Chong, R. A chemical reduction approach to the synthesis of copper nanoparticles. *Int. Nano Lett.* **2016**, *6* (1), 21–26.
- (41) Nagar, N.; Devra, V. Green synthesis and characterization of copper nanoparticles using *Azadirachta indica* leaves. *Mater. Chem. Phys.* **2018**, *213*, 44–51.
- (42) Ismail, M. Green synthesis and characterizations of copper nanoparticles. *Mater. Chem. Phys.* **2020**, *240*, 122283.
- (43) Wai, W. W.; Alkarkhi, A. F.; Easa, A. M. Optimization of pectin extraction from durian rind (*Durio zibethinus*) using response surface methodology. *J. Food Sci.* **2009**, *74* (8), C637–C641.
- (44) Mandava, K.; Kadimcharla, K.; Keesara, N. R.; Fatima, S. N.; Bommena, P.; Batchu, U. R. Green synthesis of stable copper nanoparticles and synergistic activity with antibiotics. *Indian J. Pharm. Sci.* **2017**, *79* (5), 695–700.
- (45) Singleton, V. L.; Orthofer, R.; Lamuela-Raventós, R. M., Analysis of total phenols and other oxidation substrates and antioxidants by means of folin-ciocalteu reagent. In *Methods in Enzymology*; Elsevier, 1999; Vol. 299, pp 152–178.
- (46) Lati, M.; Boughali, S.; Bouguettaia, H.; Mennouche, D.; Bechki, D.; Khemgani, M.; Mir, B. Effect of solar drying on the quality of potato. *Int. J. Sci. Res. Eng. Technol.* **2017**, *5*, 1–4.
- (47) Dananjaya, S.; Erandani, W.; Kim, C.-H.; Nikapitiya, C.; Lee, J.; De Zoysa, M. Comparative study on antifungal activities of chitosan nanoparticles and chitosan silver nano composites against *Fusarium oxysporum* species complex. *Int. J. Biol. Macromol.* **2017**, *105*, 478–488.
- (48) Wayne, P. *Performance Standards for Antimicrobial Susceptibility Testing*; Clinical and Laboratory Standards Institute (CLSI), 2010; vol 20; pp 1–5.
- (49) Naczka, M.; Shahidi, F. Extraction and analysis of phenolics in food. *J. Chromatogr. A* **2004**, *1054* (1–2), 95–111.
- (50) Pourali, O.; Asghari, F. S.; Yoshida, H. Production of phenolic compounds from rice bran biomass under subcritical water conditions. *Chem. Eng. J.* **2010**, *160* (1), 259–266.
- (51) Silva, E.; Souza, J.; Rogez, H.; Rees, J.-F.; Larondelle, Y. Antioxidant activities and polyphenolic contents of fifteen selected plant species from the Amazonian region. *Food Chem.* **2007**, *101* (3), 1012–1018.
- (52) Sinha, T.; Ahmaruzzaman, M. Green synthesis of copper nanoparticles for the efficient removal (degradation) of dye from aqueous phase. *Environmental Science and Pollution Research* **2015**, *22*, 20092–20100.
- (53) Rajagopal, G.; Nivetha, A.; Sundar, M.; Panneerselvam, T.; Murugesan, S.; Parasuraman, P.; Kumar, S.; Ilango, S.; Kunjiappan, S. Mixed phytochemicals mediated synthesis of copper nanoparticles for anticancer and larvicidal applications. *Heliyon* **2021**, *7* (6), e07360.
- (54) Sankar, R.; Manikandan, P.; Malavizhi, V.; Fathima, T.; Shivashangari, K. S.; Ravikumar, V. Green synthesis of colloidal copper oxide nanoparticles using *Carica papaya* and its application in photocatalytic dye degradation. *Spectrochimica Acta Part A: Molecular and Biomolecular Spectroscopy* **2014**, *121*, 746–750.
- (55) Djamila, B.; Eddine, L. S.; Abderrhmane, B.; Nassiba, A.; Barhoum, A. In vitro antioxidant activities of copper mixed oxide (CuO/Cu₂O) nanoparticles produced from the leaves of *Phoenix dactylifera* L. *Biomass Conversion and Biorefinery* **2022**, 1–14.
- (56) Huang, C.; Ye, W.; Liu, Q.; Qiu, X. Dispersed Cu₂O octahedrons on h-BN nanosheets for p-nitrophenol reduction. *ACS Appl. Mater. Interfaces* **2014**, *6* (16), 14469–14476.
- (57) Sathish; Rafi, S. M.; Shaik, H.; Madhavi, P.; Kosuri, Y. R.; Sattar, S. A.; Kumar, K.N. Critical investigation on Cu-O bonding configuration variation in copper-oxide thin films for low-cost solar cell applications. *Materials Science in Semiconductor Processing* **2019**, *96*, 127–131.
- (58) Sarwar, N.; Humayoun, U. B.; Kumar, M.; Zaidi, S. F. A.; Yoo, J. H.; Ali, N.; Jeong, D. I.; Lee, J. H.; Yoon, D. H. Citric acid mediated green synthesis of copper nanoparticles using cinnamon bark extract and its multifaceted applications. *Journal of Cleaner Production* **2021**, *292*, 125974.
- (59) Zhan, K.; Xia, S.; Lu, Q.; Cheng, R.; Jiang, H.; Yi, T.; Morrell, J.; Yang, L.; Xie, L.; Lei, H.; Du, G.; Gao, W. Superhydrophobic wood surface fabricated by Cu₂O nano-particles and stearic acid: its acid/alkali and wear resistance. *Holzforchung* **2021**, *75* (10), 917–931.
- (60) Faisal, S.; Jan, H.; Abdullah; Alam, I.; Rizwan, M.; Hussain, Z.; Sultana, K.; Ali, Z.; Uddin, M. N. In vivo analgesic, anti-inflammatory, and anti-diabetic screening of *Bacopa monnieri*-synthesized copper oxide nanoparticles. *ACS Omega* **2022**, *7* (5), 4071–4082.
- (61) Podstawczyk, D.; Pawłowska, A.; Bastrzyk, A.; Czeryba, M.; Oszmiański, J. Reactivity of (+)-Catechin with Copper (II) Ions: The green synthesis of size-controlled sub-10 nm copper nanoparticles. *ACS Sustain. Chem. Eng.* **2019**, *7* (20), 17535–17543.

- (62) Saratale, R. G.; Karuppusamy, I.; Saratale, G. D.; Pugazhendhi, A.; Kumar, G.; Park, Y.; Ghodake, G. S.; Bharagava, R. N.; Banu, J. R.; Shin, H. S. A comprehensive review on green nanomaterials using biological systems: Recent perception and their future applications. *Colloids Surf. B: Biointerfaces* **2018**, *170*, 20–35.
- (63) Tang, L.; Zhu, L.; Tang, F.; Yao, C.; Wang, J.; Li, L. Mild synthesis of copper nanoparticles with enhanced oxidative stability and their application in antibacterial films. *Langmuir* **2018**, *34* (48), 14570–14576.
- (64) Brumbaugh, A. D.; Cohen, K. A.; St. Angelo, S. K. Ultrasmall copper nanoparticles synthesized with a plant tea reducing agent. *ACS Sustain. Chem. Eng.* **2014**, *2* (8), 1933–1939.
- (65) Suárez-Cerda, J.; Espinoza-Gómez, H.; Alonso-Núñez, G.; Rivero, I. A.; Gochi-Ponce, Y.; Flores-López, L. Z. A green synthesis of copper nanoparticles using native cyclodextrins as stabilizing agents. *J. Saudi Chem. Soc.* **2017**, *21* (3), 341–348.
- (66) Lee, H. J.; Song, J. Y.; Kim, B. S. Biological synthesis of copper nanoparticles using *Magnolia kobus* leaf extract and their antibacterial activity. *J. Chem. Technol. Biotechnol.* **2013**, *88* (11), 1971–1977.
- (67) Abboud, Y.; Saffaj, T.; Chagraoui, A.; El Bouari, A.; Brouzi, K.; Tanane, O.; Ihssane, B. Biosynthesis, characterization and antimicrobial activity of copper oxide nanoparticles (CONPs) produced using brown alga extract (*Bifurcaria bifurcata*). *Appl. Nanosci.* **2014**, *4* (5), 571–576.
- (68) Taghavi Fardood, S.; Ramazani, A. Green synthesis and characterization of copper oxide nanoparticles using coffee powder extract. *J. Nanostruct.* **2016**, *6* (2), 167–171.
- (69) Nagar, N.; Devra, V. Green synthesis and characterization of copper nanoparticles using *Azadirachta indica* leaves. *Mater. Chem. Phys.* **2018**, *213*, 44–51.
- (70) Ghosh, M. K.; Sahu, S.; Gupta, I.; Ghorai, T. K. Green synthesis of copper nanoparticles from an extract of *Jatropha curcas* leaves: Characterization, optical properties, CT-DNA binding and photocatalytic activity. *RSC Adv.* **2020**, *10* (37), 22027–22035.
- (71) Nasrollahzadeh, M.; Mohammad Sajadi, S. Green synthesis of copper nanoparticles using *Ginkgo biloba* L. leaf extract and their catalytic activity for the Huisgen [3+2] cycloaddition of azides and alkynes at room temperature. *J. Colloid Interface Sci.* **2015**, *457*, 141–147.
- (72) Rajesh, K.; Ajitha, B.; Reddy, Y. A. K.; Suneetha, Y.; Reddy, P. S. Assisted green synthesis of copper nanoparticles using *Syzygium aromaticum* bud extract: Physical, optical and antimicrobial properties. *Optik* **2018**, *154*, 593–600.
- (73) Chung, I. M.; Abdul Rahuman, A.; Marimuthu, S.; Vishnu Kirthi, A.; Anbarasan, K.; Padmini, P.; Rajakumar, G. Green synthesis of copper nanoparticles using *Eclipta prostrata* leaves extract and their antioxidant and cytotoxic activities. *Exp. Ther. Med.* **2017**, *14* (1), 18–24.
- (74) Karki, H. S.; Shrestha, B. K.; Han, J. W.; Groth, D. E.; Barphagha, I. K.; Rush, M. C.; Melanson, R. A.; Kim, B. S.; Ham, J. H. Diversities in virulence, antifungal activity, pigmentation and DNA fingerprint among strains of *Burkholderia glumae*. *PLoS One* **2012**, *7* (9), e45376.
- (75) Messis, A.; Bettache, A.; Brahami, A.; Kecha, M.; Benallaoua, S. Optimization of antifungal production from a novel strain *Streptomyces* sp. TKJ2 using response surface methodology. *Med. Chem. Res.* **2014**, *23* (1), 310–316.
- (76) Negm, N. A.; Altalhi, A. A.; Saleh Mohamed, N. E.; Kana, M. T.; Mohamed, E. A. Growth inhibition of sulfate-reducing bacteria during gas and oil production using novel schiff base diquaternary biocides: synthesis, antimicrobial, and toxicological assessment. *ACS Omega* **2022**, *7* (44), 40098–40108.
- (77) Ngoc, U. T. P.; Nguyen, D. H. Synergistic antifungal effect of fungicide and chitosan-silver nanoparticles on *Neoscytalidium dimidiatum*. *Green Process. Synth.* **2018**, *7* (2), 132–138.
- (78) Cao, V. D.; Nguyen, P. P.; Khuong, V. Q.; Nguyen, C. K.; Nguyen, X. C.; Dang, C. H.; Tran, N. Q. Ultrafine copper nanoparticles exhibiting a powerful antifungal/killing activity against *Corticium salmonicolor*. *Bull. Korean Chem. Soc.* **2014**, *35* (9), 2645–2648.
- (79) Beltrán-Partida, E.; Valdez-Salas, B.; Valdez-Salas, E.; Pérez-Cortéz, G.; Nedev, N. Synthesis, characterization, and in situ antifungal and cytotoxicity evaluation of ascorbic acid-capped copper nanoparticles. *J. Nanomater.* **2019**, *2019*, 1.
- (80) Asghar, M. A.; Zahir, E.; Shahid, S. M.; Khan, M. N.; Asghar, M. A.; Iqbal, J.; Walker, G. Iron, copper and silver nanoparticles: Green synthesis using green and black tea leaves extracts and evaluation of antibacterial, antifungal and aflatoxin B1 adsorption activity. *Lwt* **2018**, *90*, 98–107.
- (81) Ashraf, H.; Anjum, T.; Riaz, S.; Ahmad, I. S.; Irudayaraj, J.; Javed, S.; Qaiser, U.; Naseem, S. Inhibition mechanism of green-synthesized copper oxide nanoparticles from *Cassia fistula* towards *Fusarium oxysporum* by boosting growth and defense response in tomatoes. *Environ. Sci. Nano* **2021**, *8* (6), 1729–1748.
- (82) Roy, A.; Bulut, O.; Some, S.; Mandal, A. K.; Yilmaz, M. D. Green synthesis of silver nanoparticles: biomolecule-nanoparticle organizations targeting antimicrobial activity. *RSC Adv.* **2019**, *9* (5), 2673–2702.
- (83) Rai, M.; Ingle, A. P.; Pandit, R.; Paralikar, P.; Shende, S.; Gupta, I.; Biswas, J. K.; da Silva, S. S. Copper and copper nanoparticles: Role in management of insect-pests and pathogenic microbes. *Nanotechnol. Rev.* **2018**, *7* (4), 303–315.
- (84) Pal, A.; Goswami, R.; Roy, D. N. A critical assessment on biochemical and molecular mechanisms of toxicity developed by emerging nanomaterials on important microbes. *Environ. Nanotechnol. Monit. Manag.* **2021**, *16*, 100485.
- (85) Chandrashekhara, V. D.; Lokesh, S.; V, K. V.; K, P. K. M.; Sanggonda. Potential antifungal activity of biosynthesized copper nanoparticles against *Colletotrichum Capsici* In *Chilly*. *Int. J. Biotechnol. Trends Technol.* **2021**, *11* (2), 1–7.
- (86) Muthulakshmi, L.; Varada Rajalu, A.; Kaliaraj, G. S.; Siengchin, S.; Parameswaranpillai, J.; Saraswathi, R. Preparation of cellulose/copper nanoparticles bionanocomposite films using a bioflocculant polymer as reducing agent for antibacterial and anticorrosion applications. *Compos. B: Eng.* **2019**, *175*, 107177.
- (87) Juárez-Maldonado, A.; Tortella, G.; Rubilar, O.; Fincheira, P.; Benavides-Mendoza, A. Biostimulation and toxicity: The magnitude of the impact of nanomaterials in microorganisms and plants. *J. Adv. Res.* **2021**, *31*, 113–126.